FeCrAl Layer Fabricated by DC Sputtering Enhances Pool Boiling Critical Heat Flux

Gwang Hyeok Seo [a], Hong Hyun Son [a], Gyoodong Jeun [a], Sung Joong Kim [a*]
[a] *Department of Nuclear Engineering, Hanyang University, 222 Wangsimni-ro, Seongdong-gu, Seoul 04763, Republic of Korea*
[*] *Corresponding author: sungjkim@hanyang.ac.kr*

1. Introduction

Since some severe accidents have occurred in the past several decades, the safety of nuclear reactor systems has been steadily improved to overcome a variety of limitations in the systems. Moreover, the latest lessons were learned from the Fukushima Daiich accident in 2011, which demonstrated that further advances must be made to provide more effective severe accident mitigation strategies [1]. In particular, use of Accident Tolerant Fuels (ATFs) emerged as an effective way to increase the safety margin in the reactor system [2]. For the development of ATFs, Zinkle et al. suggested three general strategies. The first and second strategies are to replace parts of the existing fuel system, specifically replacement of the current UO_2 fuel with alternative fuel forms and replacement of a Zr-based alloy cladding with an advanced cladding. The third strategy is to modify the current Zr-based alloy cladding to strengthen the oxidation resistance [3]. The former two approaches require significant design changes to the current nuclear systems including geometrical modifications. Moreover, recent studies have revealed that a practical way to modify a fuel cladding is surface coating with a high oxidation-resistant material [3-5]. Along these lines, we introduce FeCrAl deposition using a DC sputtering technique.

The sputtering technique has a distinct benefit in that it provides freedom of material selection. However, defining specific sputtering conditions to realize a FeCrAl layer that improves CHF requires a lot of effort. Many trials were conducted to find the best conditions for depositing a thin layer of FeCrAl on a stainless steel metal surface. It should be noted that although FeCrAl is oxidation-resistant, it has not been as extensively studied in the field of boiling heat transfer as pure metals or various stainless steels.

The objectives of this study were to investigate the effects of key sputtering parameters on the surface morphology of the coating and to measure pool boiling CHF in a metal heater with a FeCrAl layer. Pool boiling experiments with deionized water (DI water) at atmospheric pressure are presented. The CHF with bare stainless steel grade 316 (SS316) and FeCrAl-layered heaters are compared, and recent CHF models incorporating the surface effects are employed to elucidate the physical mechanisms for the enhanced CHF.

2. Fabrication of FeCrAl Layer on a Metal Substrate using Sputtering System

FeCrAl layers were fabricated using a DC magnetron sputtering system. A schematic image of the system is presented in Fig. 1. The vacuum chamber contains target and substrate stages. Argon (Ar) gas was used as a working gas, and it flowed through the chamber with a specific flowrate. In the chamber, the Ar plasma was excited by a constant voltage to sputter the target. The target stage attached to magnetrons was connected to a DC power supply capable of providing up to 1000 W. A bare SS316 substrate was placed on the substrate stage in the lower part of the chamber, and the substrate surface faced upward toward the target.

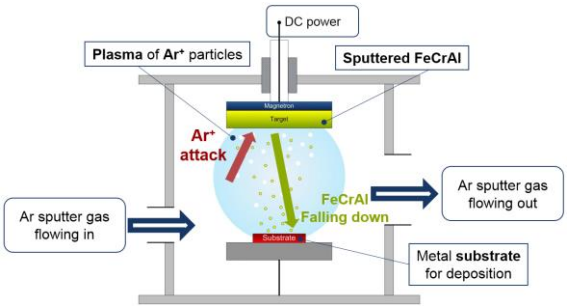

Fig. 1. Schematic of the sputtering system with Ar sputter gas

During the sputtering process, Ar ions (Ar^+) excited by a voltage sputter the target surface, and the target is bombarded with the energetic Ar^+. As a result, sputtered FeCrAl atoms from the target surface are generated and experience a sequence of collisions with the existing particles in the chamber. After a series of scattering interactions, the atoms eventually arrive at the substrate surface, which results in a final stable FeCrAl layer [6].

3. Experimental

The experiments were carried out in order to investigate the boiling behaviors of FeCrAl-layered heaters in a pool of saturated DI water under atmospheric pressure. A schematic of pool boiling facilities used in this study are shown in Fig. 2. Flat test specimens made of SS316 were used as reference bare and substrate samples for FeCrAl deposition.

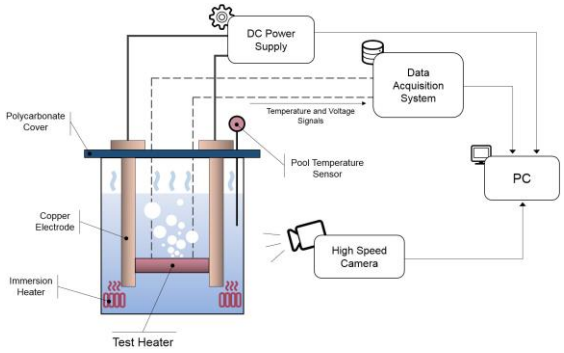

Fig. 2. Schematic of the pool boiling apparatus.

Figure 3 shows a schematic of the test heater design. The dimensions of the heating element were 35×10×2 mm^3 in length, width, and thickness, respectively. All the sides of the heater were insulated with epoxy except the central heated region. Electrical power was supplied to the copper electrodes using a DC power supply. The heater temperature was measured with a K-type thermocouple (TC) attached to the backside of the heater insulated by the epoxy.

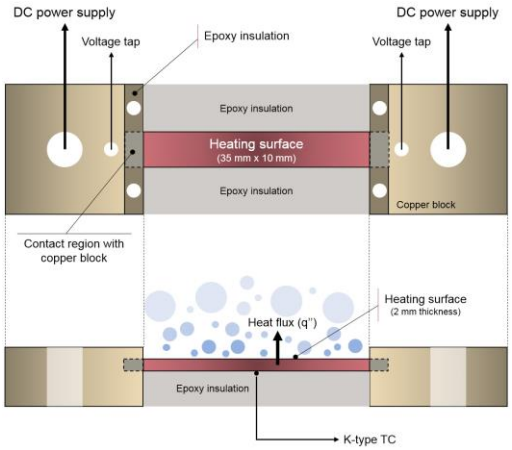

Fig. 3. Schematic of the test heater assembly.

4. Results and Discussions

4.1 Effects of Sputtering on Surface Characteristics of FeCrAl-Layered Heaters

In this study, six kinds of heater samples were prepared: one bare sample and five FeCrAl-layered samples. Among the five FeCrAl-layered samples, four FeCrAl-layered samples were fabricated with a sputtering time of 1 hour, and one sample was fabricated using a 6-hour sputtering time. The substrate temperatures in the sputtering process included room temperature (~30 ºC), 150 ºC, 300 ºC, and 600 ºC.

Figure 4 shows AFM images with corresponding surface profiles and static contact angles. The surface morphology of the FeCrAl-layered samples was significantly different from the bare sample. Generally, the roughness increased by up to 40%, compared to the bare sample. However, it is difficult to quantitatively describe the characteristics of each layer at this stage. Accordingly, a simple standardization of structural features of the sputtered layers was carried out to facilitate an understanding of the major changes in the developed pattern.

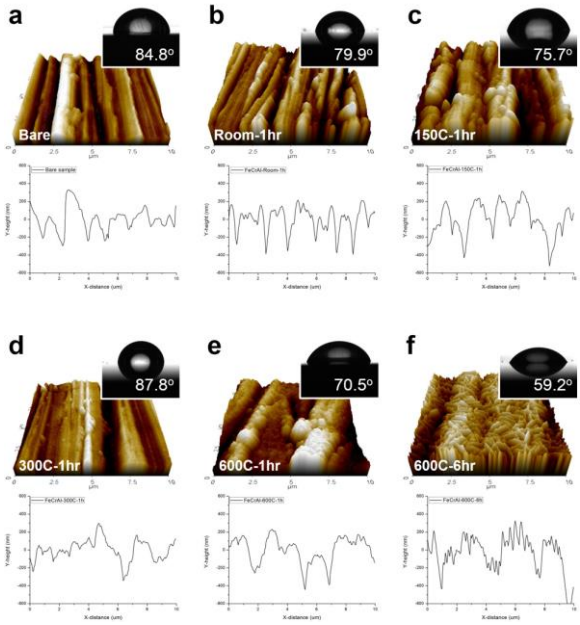

Fig. 4. AFM images with corresponding surface profiles and static contact angles.

Figure 5 exhibits simplified images of the deposition layers for each sample. The major changes in microstructures of the layer can be distinguished in terms of the width (a) and height (h) of a peak. Here, δ_{top} and δ_{bottom} represent the top and bottom widths, respectively. After sputtering, the interval between neighboring peaks generally became broader, and the heights of the peaks increased. These changes subsequently contributed to an increase in surface roughness.

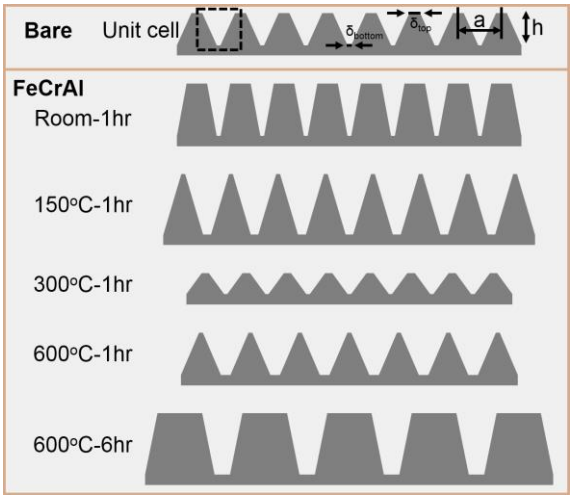

Fig. 5. Standardized structures developed on the surface at the micrometer scale.

4.2 CHF Interpretation

The CHF values from the boiling tests were compared with each other including that of the bare heater. As summarized in Table 1, CHF enhancement was observed for all FeCrAl-layered heaters as compared to the bare heater.

Table 1: Summary of CHF data.

Sample ID	CHF (Enhancement ratio) (kW/m^2)
Bare	1047±119 (1.00)
FeCrAl-Room-1hr	1258±80 (1.20)
FeCrAl-150C-1hr	1482±65 (1.42)
FeCrAl-300C-1hr	1191±175 (1.14)
FeCrAl-600C-1hr	1382±93 (1.32)
FeCrAl-600C-6hr	1207±155 (1.15)

Kandlikar's model considers surface wettability only by incorporating an apparent contact angle, which differs from the in-situ boiling parameter [7]. The model shows a limitation in predicting the CHF based on the intrinsic surface parameters. In this study, a reduction in the apparent contact angle on the sputtered layer was not significant enough to explain the observed CHF enhancement. This can be found in Fig. 6, which shows that the case with the lowest contact angle indicates a 15% CHF enhancement (here, FeCrAl-600C-6hr); however, the maximum CHF enhancement (42%, FeCrAl-150C-1hr) was observed for the case with the higher contact angle. Note that in Fig. 6, on the left y-axis, the experimental CHF ratio was defined as the ratio of the sputtering samples to that for the bare sample. On the right y-axis, the predicted CHF ratio is specified as the calculated predictions based on contact angles to that of the bare sample.

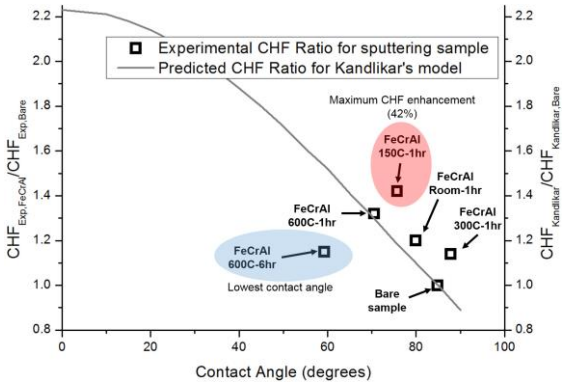

Fig. 6. Comparison of CHF ratios between the experimental data (on the right y-axis) and predictions by Kandlikar's model (on the left y-axis).

Figure 6 shows notable deviations from the predictions by Kandlikar's model. As discussed, heater substrates experienced notable changes in roughness during the sputtering process. This roughness change might induce changes in in-situ boiling parameters such as a rewetting period. Since the aforementioned models cannot explain these effects on the CHF, up-to-date CHF models incorporating roughness and rewetting periods are discussed below.

Chu et al. (2012) proposed a CHF correlation, which incorporates surface roughness using a static force balance [8]. By extending the Zuber and Kandlikar models, surface roughness and wettability were incorporated in the model as a single parameter, as shown in Eqs. (1) and (2)

$$q''_{crit} = K \cdot h_{fg} \rho_v^{1/2} \left[\sigma g \left(\rho_l - \rho_v \right) \right]^{1/4} \quad (1)$$

$$K = \left(\frac{1+\cos\beta}{16} \right) \left[\frac{2}{\pi} \frac{(1+\alpha)}{(1+\cos\beta)} + \frac{\pi}{4} (1+\cos\beta) \cos\phi \right]^{1/2} \quad (2)$$

Here, α includes roughness factor, and β and ϕ are the apparent liquid receding angle and inclined angle, respectively. Consequently, the parameter K reveals the surface effects of wettability and roughness together.

Figure 7 shows the experimental results of CHF with the FeCrAl-layered heaters. The CHF changes are compared to variations in the relative K values, which are the ratios of the data for FeCrAl-layered samples to the bare samples. The tendency of the CHF changes is in a good agreement with Chu's model. Since the K parameter implies the surface effects, the developed surface morphology of the FeCrAl layer can be critical for determining the resulting CHFs. A higher value of K indicates a greater contribution of the surface effect based on the combination of roughness factor and hydrophilicity. Obviously, the standardized images and AFM data indicated relatively flat surfaces for the samples of FeCrAl-300C-1hr and FeCrAl-600C-6hr.

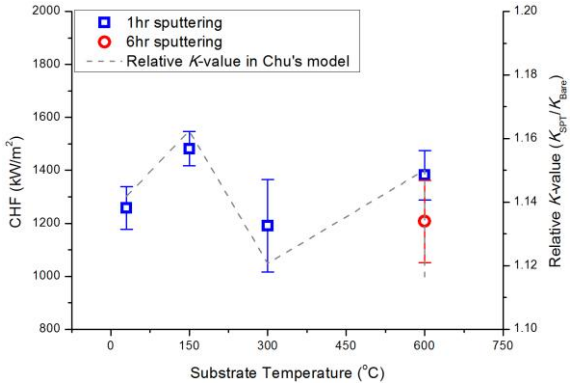

Fig. 7. Variation in CHF of the FeCrAl-layered heaters (on the left y-axis) and the relative K values (on the right y-axis) with substrate temperatures.

This improved surface effect of the FeCrAl-layered heater on CHF enhancement can be confirmed phenomenologically with a visual observation. Visualization work with the HVS was conducted to carefully capture bubble behaviors of the bare and FeCrAl-layered heaters. Figure 8 exhibits representative images of the bubbles on the heating surface of both of the samples. Another up-to-date CHF model suggested

by Dhillon et al. (2015) provides meaningful information showing how much CHF can be delayed with reduced rewetting time [9]. The amount of change in CHF was calculated using 15 msec as a reference value of the timescale from the bare sample. As the reduced rewetting time was recorded to be as long as 2 to 4 msec, the corresponding CHF enhancement was 15% to 36%. Although these are slightly lower than the experimentally observed enhancements, the trend in the CHF enhancement with FeCrAl-layered heaters is in the same direction as in Dhillon's model. Furthermore, as discussed, the improved rewetting behavior is in accordance with the surface effect predicted by Chu et al.'s model. Consequently, both the up-to-date CHF models indicate the improved surface effect, and the visual observation can be the experimental evidence for the CHF enhancement.

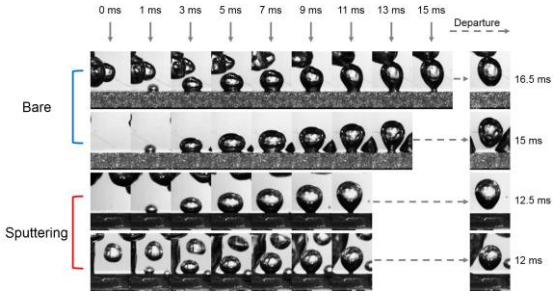

Fig. 8. High-speed images of the bubbles on the heating surface for the bare and FeCrAl-layered heater.

5. Conclusions

In this study, FeCrAl-layered heaters were fabricated using a DC sputtering process. After investigating the effects of sputtering parameters on the surface morphology, a pool boiling CHF experiment for the test heaters was performed, and experimental data were carefully compared with existing CHF predictions. The major findings observed in this study can be summarized as follows:

• The surface characteristics of the FeCrAl layer were significantly influenced by the key sputtering parameters: the substrate temperature and deposition period. Higher values of the surface roughness were observed at temperatures of 150 ºC and 600 ºC.

• The CHF enhancement was achieved for all FeCrAl-layered heaters. For the samples of FeCrAl-150C-1hr and FeCrAl-600C-1hr, higher enhancements of 42% and 32%, respectively, were observed. The trends of CHF enhancement were in a good agreement with the model of Chu et al. As the model indicates, CHF enhancement could be expected on the heating surface with a higher surface texture density, especially at the micrometer level.

• Dhillon's model proposed that a few msec reduction in the rewetting interval could enhance the CHF. The visual observation in this study confirmed a reduced rewetting interval by at least 2 msec for the FeCrAl-layered heater as compared to the bare heater.

• Finally, we confirmed that the FeCrAl layer developed by the sputtering process enhanced the thermal safety margin. Although the fabricated FeCrAl layer has the potential to enhance the thermal safety margin, further experiments are needed to demonstrate that the FeCrAl material is suitable for nuclear applications.

Acknowledgement

This research was supported by the Basic Science Research Program through the National Research Foundation of Korea (NRF) funded by the Ministry of Science, ICT & Future Planning (No. 2015R1C1A1A01054861).

REFERENCES

[1] S. Seo, Y. Lee, S. Lee, H.-Y. Kim and S. J. Kim, Effectiveness and Adverse Effects of Reactor Coolant System Depressurization Strategy with Various Severe Accident Management Guidance Entry Conditions for Opr1000, Journal of Nuclear Science and Technology, Vol. 52, pp. 695, 2014.

[2] L. J. Ott, K. R. Robb and D. Wang, Preliminary Assessment of Accident-Tolerant Fuels on Lwr Performance During Normal Operation and under Db and Bdb Accident Conditions, Journal of Nuclear Materials, Vol. 448, pp. 520, 2014.

[3] S. J. Zinkle, K. A. Terrani, J. C. Gehin, L. J. Ott and L. L. Snead, Accident Tolerant Fuels for Lwrs: A Perspective, Journal of Nuclear Materials, Vol. 448, pp. 374, 2014.

[4] K. A. Terrani, S. J. Zinkle and L. L. Snead, Advanced Oxidation-Resistant Iron-Based Alloys for Lwr Fuel Cladding, Journal of Nuclear Materials, Vol. 448, pp. 420, 2014.

[5] X. Wu, T. Kozlowski and J. D. Hales, Neutronics and Fuel Performance Evaluation of Accident Tolerant Fecral Cladding under Normal Operation Conditions, Annals of Nuclear Energy, Vol. 85, pp. 763, 2015.

[6] K. Wasa, Handbook of Sputter Deposition Technology: Fundamentals and Applications for Functional Thin Films, Nano-Materials and Mems, William Andrew, 2013.

[7] S. G. Kandlikar, A Theoretical Model to Predict Pool Boiling Chf Incorporating Effects of Contact Angle and Orientation, Journal of Heat Transfer, Vol. 123, p. 1071, 2001.

[8] K.-H. Chu, R. Enright and E. N. Wang, Structured Surfaces for Enhanced Pool Boiling Heat Transfer, Applied Physics Letters, Vol. 100, p. 241603, 2012.

[9] N. S. Dhillon, J. Buongiorno and K. K. Varanasi, Critical Heat Flux Maxima During Boiling Crisis on Textured Surfaces, Nat Commun, Vol. 6, p. 8247, 2015.